

# Institutionen för systemteknik

## Department of Electrical Engineering

**Examensarbete**

### **Parallel Hybridization of a Heavy-Duty Long Hauler**

Examensarbete utfört i Fordonssystem  
vid Tekniska högskolan vid Linköpings universitet  
av

**Tommie Eriksson**

LiTH-ISY-EX-15/4881-SE

Linköping 2015



**Linköpings universitet**  
**TEKNISKA HÖGSKOLAN**



# Parallel Hybridization of a Heavy-Duty Long Hauler

Examensarbete utfört i Fordonssystem  
vid Tekniska högskolan vid Linköpings universitet  
av

**Tommie Eriksson**

LiTH-ISY-EX-15/4881-SE

Handledare: **Ph.D. Student Xavier Llamas Comellas**  
ISY, Linköpings universitet

**Per Rosander**  
Lead Engineer-Analysis, AVL

Examinator: **Associate Professor Lars Eriksson**  
ISY, Linköpings universitet

Linköping, 18 juni 2015



	<b>Avdelning, Institution</b> Division, Department	<b>Datum</b> Date
	Division of Vehicular Systems Department of Electrical Engineering SE-581 83 Linköping	2015-06-18

<b>Språk</b> Language <input type="checkbox"/> Svenska/Swedish <input checked="" type="checkbox"/> Engelska/English <input type="checkbox"/> _____	<b>Rapporttyp</b> Report category <input type="checkbox"/> Licentiatavhandling <input checked="" type="checkbox"/> Examensarbete <input type="checkbox"/> C-uppsats <input type="checkbox"/> D-uppsats <input type="checkbox"/> Övrig rapport <input type="checkbox"/> _____	<b>ISBN</b> _____ <b>ISRN</b> LiTH-ISY-EX-15/4881-SE <b>Serietitel och serienummer</b> <b>ISSN</b> Title of series, numbering                      _____
--	---	---

**URL för elektronisk version**

<http://urn.kb.se/resolve?urn=urn:nbn:se:liu:diva-119884>

<b>Titel</b> Title	Parallell hybridisering av en tung långträdare Parallel Hybridization of a Heavy-Duty Long Hauler
<b>Författare</b> Author	Tommie Eriksson

**Sammanfattning**  
Abstract

Long haulage of heavy-duty trucks weighing over 15-ton stands for nearly 50% of the fuel consumption among trucks, making them the most fuel consuming category. This indicates the potential benefits in improving the fuel efficiency for said category. Hybridization is one possible solution.

Hybrid vehicles are vehicles with two or more power sources in the powertrain. Different powertrain configurations, hybridization levels and hybrid concepts are best suited for different applications. With prices for fossil fuels constantly rising hybridization is an important technology to improve fuel efficiency.

Different variations of configurations and concepts enables many choices when deciding on a hybrid driveline. A simulation tool for efficiently comparing various hybrid drivelines would be a great asset when deciding on a configuration for a certain vehicle application. For this thesis the application in focus is the previously mentioned category, a heavy duty long hauler weighing 36-ton.

The modeling approach used for the simulation tool is called quasistatic modeling or "backward modeling". This name comes from, based on a chosen drive cycle, the resisting forces which act on the vehicle can statically be calculated at each step from the velocity profile. The required power to drive along the drive cycle can then be calculated backwards within the powertrain resulting in a fuel consumption for the combustion engine. For this the free QSS-toolbox for Matlab Simulink has been used as a base and modified when needed.

The configuration chosen to be implemented is a parallel electric hybrid and was chosen for its good characteristics for the type of driving highways provide. For this configuration two types of controllers are used, one being an Equivalent Consumption Minimization Strategy controller and the other a simple, rule based heuristic controller.

The results for both controllers show small benefits with hybridization of the long hauler compared with the conventional which in the long run would make bigger difference because of the large consumption in whole. A sensitivity analysis was also done showing that improving conventional vehicle parameters can be as beneficial as hybridization.

<b>Nyckelord</b> Keywords	Long Haul, Heavy Duty, Hybrid Electric Vehicle, Parallel, QSS, Simulink
------------------------------	---



## Abstract

Long haulage of heavy-duty trucks weighing over 15-ton stands for nearly 50% of the fuel consumption among trucks, making them the most fuel consuming category. This indicates the potential benefits in improving the fuel efficiency for said category. Hybridization is one possible solution.

Hybrid vehicles are vehicles with two or more power sources in the powertrain. Different powertrain configurations, hybridization levels and hybrid concepts are best suited for different applications. With prices for fossil fuels constantly rising hybridization is an important technology to improve fuel efficiency.

Different variations of configurations and concepts enables many choices when deciding on a hybrid driveline. A simulation tool for efficiently comparing various hybrid drivelines would be a great asset when deciding on a configuration for a certain vehicle application. For this thesis the application in focus is the previously mentioned category, a heavy duty long hauler weighing 36-ton.

The modeling approach used for the simulation tool is called quasistatic modeling or "backward modeling". This name comes from, based on a chosen drive cycle, the resisting forces which act on the vehicle can statically be calculated at each step from the velocity profile. The required power to drive along the drive cycle can then be calculated backwards within the powertrain resulting in a fuel consumption for the combustion engine. For this the free QSS-toolbox for Matlab Simulink has been used as a base and modified when needed.

The configuration chosen to be implemented is a parallel electric hybrid and was chosen for its good characteristics for the type of driving highways provide. For this configuration two types of controllers are used, one being an Equivalent Consumption Minimization Strategy controller and the other a simple, rule based heuristic controller.

The results for both controllers show small benefits with hybridization of the long hauler compared with the conventional which in the long run would make bigger difference because of the large consumption in whole. A sensitivity analysis was also done showing that improving conventional vehicle parameters can be as beneficial as hybridization.



## Acknowledgments

From ISY, department of Vehicular Systems at Linköping University, I would like to thank my examiner Associate Professor Lars Eriksson for giving me the opportunity to do my thesis at the vehicular system division. A special thanks to my supervisor, Ph.D. Student Xavier Llamas Comellas, for his help, quick feedback and excellent suggestions on improving this thesis.

At AVL I would like to thank my supervisor Per Rosander for his help and advice throughout this thesis. I also would like to thank Sarah Zitouni for her tremendous support and feedback on this report and always being there when needed. Further, I want to thank everyone in the AVL office for welcoming me and all the fun times had and fun times to come.

Last but not least I want to thank my family and friends for their support throughout all my years studying. Thanks for always being there!

*Linköping, Juni 2015  
Tommy Eriksson*



---

# Contents

<b>1</b>	<b>Introduction</b>	<b>1</b>
1.1	Background . . . . .	1
1.2	Purpose and goal . . . . .	3
1.3	Introduction of Hybrid Powertrains . . . . .	3
1.3.1	Series . . . . .	3
1.3.2	Parallel . . . . .	4
1.3.3	Series-parallel . . . . .	5
1.4	Problem formulation . . . . .	6
1.5	Related research . . . . .	6
1.6	Expected results . . . . .	7
<b>2</b>	<b>Models</b>	<b>9</b>
2.1	Drive Cycle . . . . .	10
2.2	Longitudinal Vehicle Model . . . . .	11
2.3	Gear Box . . . . .	13
2.4	Combustion Engine . . . . .	14
2.5	Battery . . . . .	15
2.6	Electric Motor/Generator . . . . .	16
<b>3</b>	<b>Long Hauler Configurations</b>	<b>19</b>
3.1	Conventional Long Hauler . . . . .	19
3.1.1	Vehicle parameters . . . . .	19
3.1.2	Gear Box . . . . .	20
3.1.3	Combustion Engine . . . . .	20
3.2	Parallel Hybrid Long Hauler . . . . .	21
3.2.1	Downsizing . . . . .	21
3.2.2	Electric sizing . . . . .	22
<b>4</b>	<b>Controller</b>	<b>25</b>
4.1	Equivalent Consumption Minimization Strategy . . . . .	25
4.2	Heuristic Controller . . . . .	28
<b>5</b>	<b>Results</b>	<b>31</b>

---

5.1	Conventional . . . . .	31
5.2	Longitudinal Vehicle Model . . . . .	32
5.3	Gear Box . . . . .	33
5.3.1	Gear Shifting . . . . .	33
5.4	Combustion Engine . . . . .	34
5.5	Fuel Consumption . . . . .	35
5.6	Parallel Hybrid . . . . .	35
5.6.1	Downsized Combustion Engine . . . . .	36
5.6.2	Electric Motor . . . . .	37
5.7	Fuel Consumption . . . . .	38
5.7.1	ECMS Controller . . . . .	38
5.7.2	Heuristic Controller . . . . .	43
5.8	Sensitivity analysis . . . . .	46
<b>6</b>	<b>Conclusions</b>	<b>49</b>
6.1	Future Work . . . . .	49
	<b>Bibliography</b>	<b>51</b>

# 1

---

## Introduction

### 1.1 Background

Long haulage of trucks weighing over 15-ton (class 8) are the most fuel consuming category of trucks [1] and stands for nearly 50% of the fuel consumption among trucks. This indicates the potential benefits in improving the fuel efficiency for said category. With prices for fossil fuels constantly rising [2] hybridization is an important technology to improve fuel efficiency.

Hybrid vehicles are vehicles with two or more power sources in the powertrain [3]. Different powertrain configurations, hybridization levels and hybrid concepts are best suited for different applications. The key advantages with a hybrid powertrain is firstly the possibility to implement some kind of KERS (Kinetic Energy Recovery System) which gives the possibility to recuperate and reuse some of the energy otherwise dissipated and lost when using regular friction brakes. Another advantage is the ability to split the required torque and thus allowing the combustion engine to run in a more efficient operation point. Lastly, with a hybrid powertrain it is also possible to downsize the combustion engine since they are over dimensioned for normal driving conditions due to the acceleration demands.

Commercial vehicles can be classified in eight different classes depending on their weight. In Figure 1.1 from [3] the eight classes are shown. This thesis will focus on the hybridization of a class 8 (over 15-ton) long hauler.

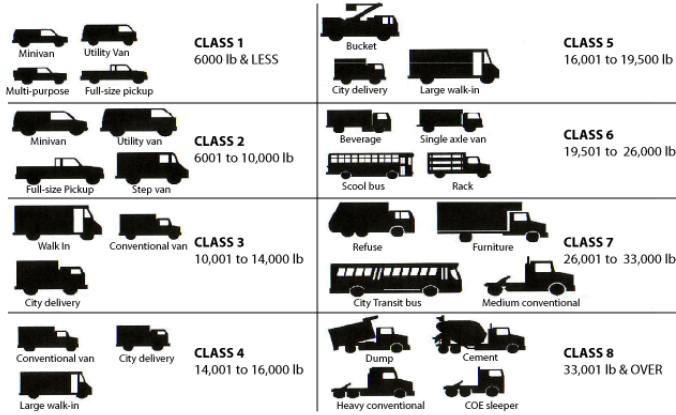


**Figure 1.1:** Commercial vehicle classifications by the Federal Highway Administration (FHWA).

For a heavy truck when traveling in a downhill slope the gravity will eventually start to assist the truck and give the necessary energy to maintain a constant speed (coasting). A simple calculation, using vehicle parameters from Chapter 3 and equations for the required tractive force in [4] results in Figure 1.2, where one can see the required tractive power w.r.t. slope percentage for a 36-ton heavy truck traveling at constant speed 85km/h. The figure shows there is power available for recuperation when running in downhill slopes just above 1.5%, which otherwise would be lost in the brakes. In these cases this energy can, minus the power transformation losses, be recuperated. The benefits of this possibility will be investigated in this thesis.

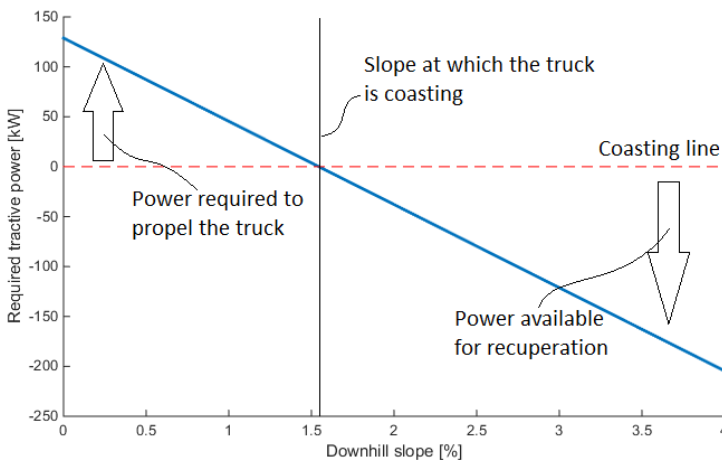


**Figure 1.2:** Tractive power for a 36-ton Heavy Truck in 85 km/h

## 1.2 Purpose and goal

The purpose of the thesis is to optimize the hybrid powertrain configuration of a heavy duty long hauler and compare to a conventional long hauler. To do this, models for the vehicle, gear box, engine, electric generator/motor, battery will be used. From AVL side the final goal is to have a simulation tool which they can use to compare different configurations and concepts of hybridized powertrains as material for early decisions during development phases.

## 1.3 Introduction of Hybrid Powertrains

A hybrid vehicle is a vehicle with two or more power sources. There are different types of hybrid concepts which uses different kinds of energy storage. In commercial vehicles the following are [3]

- \* Electric
- \* Hydraulic
- \* Pneumatic
- \* Mechanic

The hydraulic, pneumatic and mechanical concepts are more appropriate for applications with frequent start and stops since they have the ability to charge and discharge a larger amount of power (large power density) but lack the ability to store large quantities of energy (low energy density). The electric concept has the opposite properties. It is then the most beneficial storage type for the long haul application and will therefore be the targeted type. One kind of electric hybrid is the plug-in electric hybrid, PHEV, which has the ability to charge the battery from an external source. A PHEV has a larger battery than a regular HEV and the ability to drive larger distances in pure electric mode.

For the hybrid electric vehicles, HEVs, there are different types of configurations which differ in the way the prime movers are coupled. The most common types are [3]

- \* Series
- \* Parallel
- \* Series-parallel

### 1.3.1 Series

In the series hybrid the combustion engine (CE) is connected to a generator (GEN) which charges the battery (BAT) through a power converter (P). The vehicle is then propelled with an electric motor (EM) through the gear box (GB). The combustion engine is hence de-coupled from the wheels which gives it an extra degree of freedom, the engine speed, which enables it to run at a more efficient point. The series hybrid have four different modes:

1. Pure electric drive
2. Battery recharging
3. Hybrid drive
4. Regenerative braking

In pure electric drive only the battery is used as power source. In battery charging the combustion engine is used at its maximum efficiency allowing the excess power to charge the battery. The hybrid drive is when both sources produce the power to propel the vehicle. During the regenerative braking the kinetic energy is recuperated by the electric motor acting as a generator. Figure 1.3 shows a sketch of the topology of a series hybrid. This configuration is best suited for start and stop applications like city buses and disposal/delivery trucks. When driven on a highway at a higher velocity there are a double conversion from mechanic  $\rightarrow$  electric  $\rightarrow$  mechanic in the series making it less efficient.

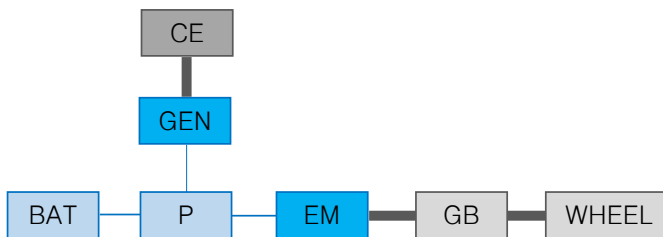


**Figure 1.3:** *Topology of a series hybrid. Bold lines represent mechanical links and thin lines electric links*

Another disadvantage with a series is the need for a bigger electric motor and battery to be able to act as main mover. This adds weight and production costs to the vehicle.

### 1.3.2 Parallel

In the parallel hybrid both the combustion engine (CE) and the electric motor (EM) are coupled to the wheels through the gear box (GB). The battery (BAT) is only connected to the electric motor through a power converter (P). The parallel hybrid configuration in Figure 1.4 allows for five modes:

1. Conventional drive
2. Power assist
3. Battery recharging
4. Pure electric drive

## 5. Regenerative braking

The conventional drive is when the vehicle is only propelled by the combustion engine. The power assist is used when the combustion engine cannot deliver a sufficient amount of power, the electric motor then acts as help. In battery charging the combustion engine is used at its maximum efficiency allowing the excess power to charge the battery. In pure electric drive the vehicle is propelled by the electric motor. In regenerative braking the kinetic energy is recuperated by the electric motor acting as a generator.

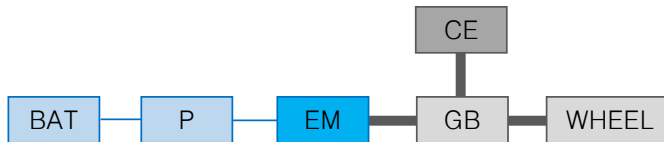


**Figure 1.4:** *Topology of a parallel hybrid. Bold lines represent mechanical links and thin lines electric links*

The benefits from a parallel hybrid is the ability to size the electric components after the need depending on how much the combustion engine is downsized. The parallel is also an easier system to control regarding the torque split. A drawback with the parallel is the coupled link between the electric motor, the combustion engine and gearbox, which hinders the combustion engine to charge the battery at standstill.

### 1.3.3 Series-parallel

The series-parallel has one combustion engine (CE) and two electric motors where one acts as a motor (EM) and the other as a generator (GEN). For the series-parallel configuration a common solution is to use a planetary gear set (PGS), shown in 1.5. This allows the powertrain to utilize the benefits of a parallel when driving on a highway and the benefits of a series in city traffic. The drawback of the series-parallel is that it is more complex.

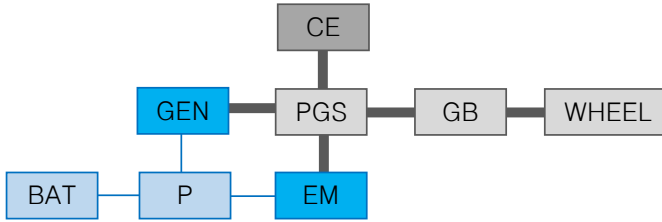


*Figure 1.5: Topology of a series-parallel hybrid. Bold lines represent mechanical links and thin lines electric links*

## 1.4 Problem formulation

Different variations of configurations and concepts enables many choices when deciding on a hybrid powertrain. A simulation tool for efficiently comparing various hybrid powertrains would be a great asset when deciding on a configuration for a certain vehicle application. A part of this thesis is also to find which powertrain parameters are most relevant for having an accurate enough model. For this thesis the main focus is on a heavy duty long hauler. The hybrid configuration will then be optimized and compared with the conventional long hauler.

Besides, it is of interest that the simulation tool should be flexible so that other applications can be investigated and compared without too much added work.

## 1.5 Related research

When reviewing the existent literature, it has been found that much of the research done is made for other applications with frequent stop and start cycles where there is most to gain from regenerative braking. Such applications are for example city buses, disposal trucks and step vans. In [5] a comparison between series and parallel with plug-in and non-plug-in configurations was made for a 6.4-ton step van resulting in a remarkable 168% improvement in miles per gallon for the parallel plug-in configuration on a certain drive cycle. Another study is [6] where it is shown that, for a small 2.5 ton truck, 62% of the braking energy can be returned to the kinetic energy of the vehicle.

A study investigating long haulage is a thesis from Chalmers University [7] where a predictive energy management for a parallel electric mild hybrid was developed and studied. With the hybrid set-ups used fuel savings near 4% compared to the conventional were achieved.

Further, in the fourth publication in the dissertation of Erik Hellström [8], he studies the management of kinetic and electric energy to be used in the look-ahead control of a heavy trucks. Simulations on three parallel electric hybrids with increasing size on electric motor results in the conclusion that a modestly sized electrical system achieves most gain. This is due to the increased resisting

forces resulting from the added mass from the electric components and higher mean velocity achieved with the hybrid.

Moreover, in [9] the hybridization of a class-8 long hauler is analysed for two different configurations. In this study the results are compared to the conventional and by simulations with a drive cycle that has hills every certain distance it is shown that hybridization is beneficial in hilly terrain.

A new thinking approach was made in [10] where an electric motor was implemented in the trailer in series with the parallel hybrid electric truck to increase the amount of recoverable brake energy. With this self propelling trailer there was also an increased tractor-trailer stability because of the capability of torque vectoring which is an active yaw control.

In [11] class-8 trucks technologies are analysed for fuel savings and economics. In the study non-electric future improvements like reduced air drag, rolling resistance etc. are made and compared with the existing conventional truck.

Later, electric hybridization of the truck is analyzed with different sizing of the electric motor and battery packs with the conclusion that for long haul applications there is a small fuel improvement but from a economic perspective the non-electric improvements are more beneficial. Nevertheless, this study neglected the effects of altitude changes where other studies taking it in account have shown the hybridization to be the most effective way.

## 1.6 Expected results

From the literature and articles regarding hybridization and its possible benefits, especially reading [9], the expected results from this thesis is that minor fuel economy savings will be achieved and will be very depending on the amount of altitude variations. On totally flat roads and at higher loads given by highways, a combustion engine already operates in a very efficient point and hybridization may not contribute to an increased fuel efficiency.



# 2

## Models

In this thesis, the components within the powertrain are modeled separately and are connected through the link of power flow from each component to the next. The modeling approach is called quasistatic modeling or "backward modeling". This name comes from, based on a chosen drive cycle, described in section 2.1, the resisting forces which act on the vehicle can statically be calculated at each step from the velocity profile. The required power to drive along the drive cycle can then be calculated backwards within the powertrain resulting in a fuel consumption  $m_f$  for the combustion engine. This chain of calculations is shown in Figure 2.1. The free QSS-toolbox for Matlab Simulink [12] has been used as a base and has been modified when needed. In Table 2.1, the physical parameters used in the modeling are described.

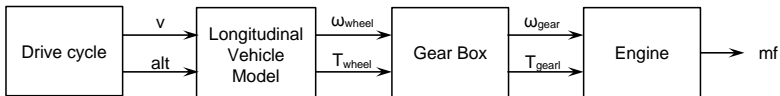


**Figure 2.1:** Powerflow in backward modeling.

Parameter	Denomination	Value	Unit
Air density	$\rho_{air}$	1.18	kg/m <sup>3</sup>
Diesel density	$\rho_{diesel}$	832	kg/m <sup>3</sup>
Diesel lower heating value	$q_{LHV}$	43.4	MJ/kg
Gravitational acceleration	$g$	9.81	m/s <sup>2</sup>

**Table 2.1:** Physical parameters

## 2.1 Drive Cycle

The drive cycles consist of data for time, velocity profile and elevation profile. The drive cycles used are in Table 2.2 and they are extracted from the road between Lyon and Clermont in France. To obtain different elevation profiles the cycles' altitude were scaled and the velocity profile accordingly. The drive cycle depicted in Figure 2.2 is the hilliest cycle, LC\_8.

With this data, one can easily obtain the average velocity (2.1), the acceleration (2.2), the driven distance (2.3) and the road inclination (2.4). These are assumed to be constant during the step size  $h$  which here is set to 1 second. The drive cycle is a very important part of the quasistatic simulation when evaluating a configuration for a certain application.

$$\bar{v}_i = \frac{v_{i+1} + v_i}{2} \quad (2.1)$$

$$\bar{a}_i = \frac{v_{i+1} - v_i}{h} \quad (2.2)$$

The total distance driven is the sum of all velocity steps multiplied with the step size  $h$  for all  $N$  steps.

$$x_{tot} = \sum_{i=0}^N v_i \cdot h \quad (2.3)$$

The inclination at each step in radians is calculated with simple trigonometry.

$$\alpha_{incl} = \tan\left(\frac{alt_{i+1} - alt_i}{\bar{v}_i \cdot h}\right) \quad (2.4)$$

Cycle	Top Elevation
LC_1	0 m
LC_2	25 m
LC_3	50 m
LC_4	140 m
LC_5	190 m
LC_6	235 m
LC_7	280 m
LC_8	375 m

**Table 2.2:** The drive cycles used for the simulation of the models.

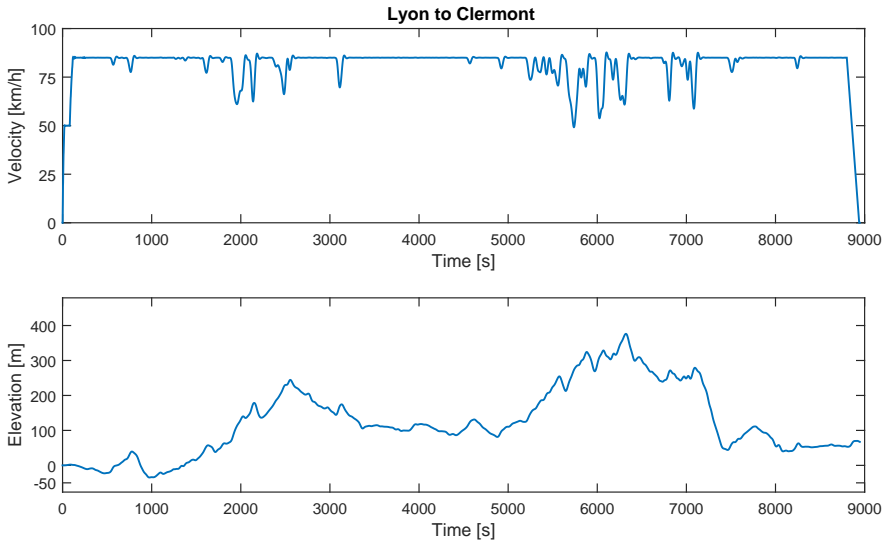


**Figure 2.2:** Plot of the hilliest Lyon to Clermont drive cycle (LC\_8). The velocity profile in the upper subplot and the elevation profile in the lower.

## 2.2 Longitudinal Vehicle Model

The longitudinal model consists of two resisting forces, the gravitational force and a tractive force. The tractive force at the wheels is produced by the powertrain.

The forces are shown in Figure 2.3. The two resisting forces are the aerodynamic resistance and the rolling resistance. The gravitation acts as a pulling force when going uphill, pushing when going downhill.

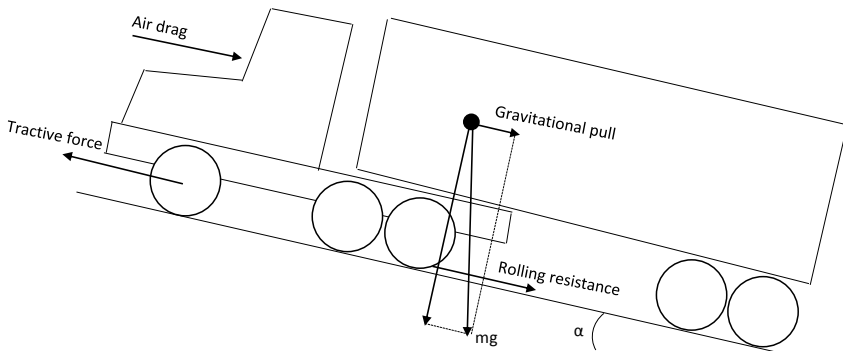


**Figure 2.3:** Acting forces on the long hauler

The longitudinal dynamics of the long hauler is modeled with Newton's second law of motion as follows

$$m_{lh} \cdot a = F_{trac} - (F_{air} + F_{roll} + F_{gravity}) \quad (2.5)$$

Following are the models of the resisting forces and the parameters influencing these are summarized in Table 2.3.

Parameter	Denomination	Unit
Frontal area	$A_f$	$m^2$
Drag coefficient	$c_d$	-
Rolling resistance coefficient	$c_r$	-
Total long hauler mass	$m_{lh}$	kg
Wheel radius	$r_w$	m

*Table 2.3: Vehicle parameters for the long hauler*

## Aerodynamic Resistance

The aerodynamic resistance is modeled with the long hauler as a prismatic body with a frontal area  $A_f$  and an aerodynamic drag coefficient  $c_d$  which is assumed to be constant [4]. The aerodynamic resistance  $F_{air}$  can be seen as the amount of energy needed to press the air aside and its expression is

$$F_{air} = \frac{1}{2} \cdot \rho_{air} \cdot A_f \cdot c_d \cdot v^2 \quad (2.6)$$

where  $v$  is the velocity of the vehicle and  $\rho_{air}$  the air density.

## Rolling Resistance

The rolling resistance  $F_{roll}$  is modeled as in (2.7) where the rolling friction coefficient  $c_r$  can depend on many variables such as vehicle speed, tire pressure, temperature and road surface. For this application since it is meant for a simple early model and the vehicle speed is within moderate limits it will be assumed constant [13].

$$F_{roll} = m_{lh} \cdot g \cdot c_r \cdot \cos(\alpha_{incl}), \quad v > 0 \quad (2.7)$$

with  $\alpha_{incl}$  being the slope and  $m_{lh}$  the total mass of the long hauler.

## Gravitation

For a heavy long hauler it is clear that the major resisting force when going in a uphill slope is the gravitational force. The gravitational force  $F_{gravity}$  acting on the longitudinal model is achieved with simple trigonometry as

$$F_{gravity} = m_{lh} \cdot g \cdot \sin(\alpha_{incl}) \quad (2.8)$$

## Required Power

The required force  $F_{req}$  is then the tractive force  $F_{trac}$  from (2.5) and thus the required power to propel the long hauler at a certain velocity  $v$  is calculated with (2.11). The velocity and acceleration are given from (2.1) and (2.2).

$$F_{req} = F_{trac} = m_{lh} \cdot a + F_{air} + F_{roll} + F_{gravity} \quad (2.9)$$

$$T_{req} = F_{req} \cdot r_w \quad (2.10)$$

$$P_{req} = T_{req} \cdot \omega_w = T_{req} \cdot \frac{v}{r_w} \quad (2.11)$$

Substituting (2.9) and (2.10) in (2.11) yields the expression

$$P_{req} = (m_{lh} \cdot a + F_{air} + F_{roll} + F_{gravity}) \cdot v \quad (2.12)$$

## 2.3 Gear Box

For the long hauler a manual gear box has been chosen and the power flow in the gear box is modeled with an efficiency  $\eta_{gb}$  and an idle power loss  $P_{idle,gb}$  as follows

$$P_{gb} = \eta_{gb} \cdot P_{req} - P_{idle,gb} \quad (2.13)$$

This means that the required input torque and angular speed from the gear box is given as follows

$$T_{gb} = \frac{T_w}{\gamma_{gb}} \cdot \eta_{gb}^{\text{sign}(-T_w)} \quad \omega_{gb} = \gamma_{gb} \cdot \omega_w \quad (2.14)$$

where the 'sign' gives the right torque conversion depending on the power flows direction.

$$\begin{cases} T_w > 0 & \text{provide power} \\ T_w < 0 & \text{recover power} \end{cases}$$

## Gear Selection

The gear selection is controlled only by the vehicle speed. Since highway roads are the main target, suboptimal gear changing will not make a huge impact and the long hauler will mainly be driven on the highest gear available.

## 2.4 Combustion Engine

The combustion engine model from the QSS-toolbox [12] uses the Willan's Line approximation (2.15). This approximation uses the brake mean effective pressure  $p_{me}$  and this results in an independence of engine size in the model.

$$p_{me} = e \cdot p_{mf} - p_{me0} \quad (2.15)$$

where  $e$  is the indicated efficiency,  $p_{mf}$  the fuel mean effective pressure and  $p_{me0}$  the losses.  $p_{me}$  is a formulation of the engine torque and efficiency normalized with the displacement volume  $V_d$ .

$$p_{me} = \frac{T_{ce} \cdot 4\pi}{V_d} \quad (2.16)$$

The fuel mean effective pressure  $p_{mf}$  is defined in (2.17). For a four-stroke engine,  $p_{me}$  is the pressure which in one full expansion stroke has to act on the piston in order to produce the same amount of work as two revolutions in a real engine.

$p_{mf}$  is the mean effective pressure an engine with 100% efficiency would produce, hence (2.18) describes the engine's efficiency.

$$p_{mf} = \frac{m_f \cdot q_{LHV}}{V_d} \quad (2.17)$$

$$\eta_{ce} = \frac{p_{me}}{p_{mf}} \quad (2.18)$$

The engine losses  $p_{me0}$  consists of a gas exchange loss  $p_{me0,g}$  and friction loss  $p_{me0,f}$ . The gas exchange loss is assumed constant and the friction is modeled as the ETH friction model [12] in (2.20) with the friction coefficients  $k_1$ ,  $k_2$ ,  $k_3$  and  $k_4$  for the diesel engine in Table 2.4.

$$p_{me0} = p_{me0,g} + p_{me0,f} \quad (2.19)$$

$$p_{me0,f} = k_1(k_2 + k_3 \cdot S^2 \cdot \omega_{ce}^2) \Pi_{max} \cdot \sqrt{\frac{k_4}{B}} \quad (2.20)$$

where  $\omega_{ce}$  is the engine speed,  $S$  and  $B$  being the stroke and bore of the cylinder and  $\Pi_{max}$  the maximum boost ratio which for a naturally aspirated engine is 1.

Further, the power that the engine produces can now be calculated as

$$P_{ce} = \frac{P_{gb}}{\eta_{ce}} \quad (2.21)$$

where  $P_{gb}$  is the required input power to the gear box.

Finally, the fuel mass can be calculated using the lower heating value for diesel and integrating for each time step.

$$m_f = \sum_{i=0}^N \frac{P_{ce}(i)}{q_{LHV}} \quad (2.22)$$

The fuel consumption is then obtained with the density of diesel  $\rho_{diesel}$  and the total traveled distance  $x_{tot}$ .

$$V_{liter} = \frac{10^5 \cdot m_f}{\rho_{diesel} \cdot x_{tot}} \quad [l/100km] \quad (2.23)$$

Willan parameters	Denomination	Value	Unit
Indicated efficiency	$e$	0.4	-
Friction coefficient 1	$k_1$	$1.44 \cdot 10^5$	Pa
Friction coefficient 2	$k_2$	0.5	-
Friction coefficient 3	$k_3$	$1.1 \cdot 10^{-3}$	$s^2 \cdot m^2$
Friction coefficient 4	$k_4$	0.0075	m
Maximum boost ratio	$\Pi_{max}$	1	-

**Table 2.4:** Willan parameters for the diesel engine

## 2.5 Battery

The battery is a complex system to model. For a battery to be properly modeled, data on its charge and discharge is needed. Without these data the battery model can be approximated by using an equivalent circuit, described in [4], with constant values for the parameters in Table 2.5. Added weight is calculated with the ratio 180 Wh/kg from [4].

Parameter	Denomination	Unit
Battery power	$P_{bat}$	W
Battery voltage	$U_{bat}$	V
Open circuit voltage	$U_{oc}$	V
Inner resistance	$R_i$	$\Omega$
Current	$I_{bat}$	A

**Table 2.5:** Battery parameters

The equivalent circuit is a very simplified physical model but gives a sufficient representation for the task. The battery is modeled with an ideal voltage source in series with an internal resistance, as shown in Figure 2.4, where the open circuit voltage  $U_{oc}$  acts as the equilibrium for the battery potential. With Kirchhoff's voltage law (2.24) the battery voltage  $U_{bat}$  can be calculated as follows

$$U_{bat} = U_{oc} - R_i \cdot I_{bat} \quad (2.24)$$

With the trivial relationship  $P = U \cdot I$ , the battery power can be written as in (2.25) where the term " $-R_i \cdot I_{bat}^2$ " represents the losses within the battery and depends only on the current.

$$P_{bat} = U_{oc} \cdot I_{bat} - R_i \cdot I_{bat}^2 \quad (2.25)$$

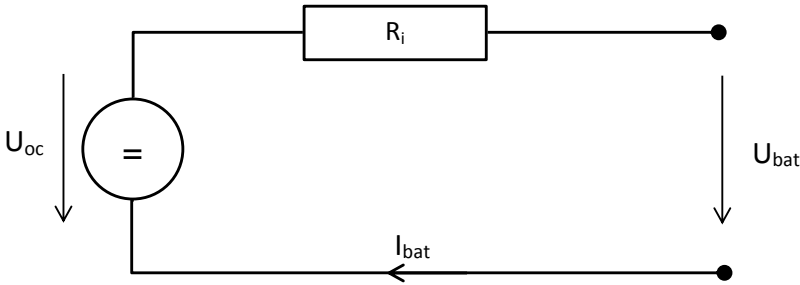


**Figure 2.4:** Equivalent circuit of a battery.

## State of Charge

The state of charge,  $q$ , of a battery is the ratio between the available battery charge  $Q$  and the nominal capacity of the battery  $Q_0$ .

$$q = \frac{Q}{Q_0} \quad (2.26)$$

The battery charge is hard to measure directly but the variation in battery charge can be approximated with (2.27) which yields to (2.28)

$$\dot{Q} = -I_{bat} \quad (2.27)$$

$$\dot{q} = \frac{\dot{Q}}{Q_0} = -\frac{I_{bat}}{Q_0} \quad (2.28)$$

## 2.6 Electric Motor/Generator

The electric motor model from the QSS-toolbox [12] is based on a scalable efficiency map and torque curve. The efficiency map is shown in Figure 2.5 where the first quadrant gives the efficiency for the motor as a mover and the second quadrant the motor's efficiency as a generator. The map is constructed to be independent of the power flow's direction and the required power to the electric motor is obtained by

$$P_{em} = \eta_{em}(\omega_{em}, T_{em}) \cdot \omega_{em} \cdot T_{em} \quad (2.29)$$

$T_{em}$  being the torque desired from the electric motor,  $\omega_{em}$  the angular velocity of the motor. With the efficiency map  $P_{em}$  is then the power required from the battery.

A scale factor of 1 yields the maximum torque and power curve represented in Figure 2.6. Added weight from the electric motor is calculated with the weight to power ratio 1.5 kg/kW from [14].

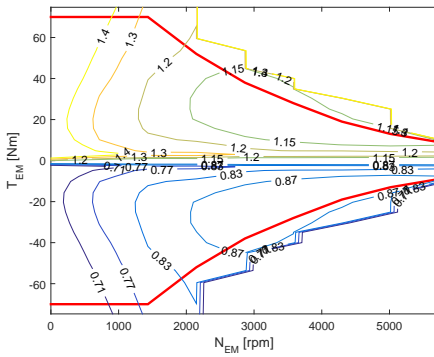


**Figure 2.5:** Efficiency map for the electric motor.

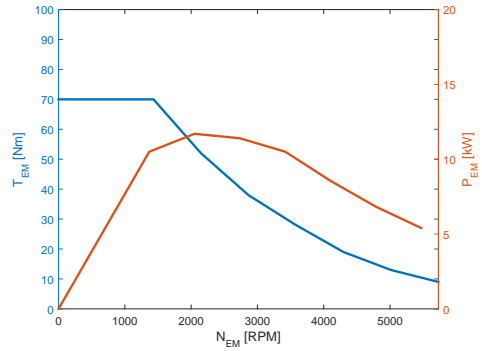


**Figure 2.6:** Torque and power curve for the electric motor with the scale factor set to 1.



# 3

---

## Long Hauler Configurations

In this chapter the different configurations for the long hauler are discussed and parameter choices motivated. The results from the simulations of the models are analysed and discussed in Chapter 5.

### 3.1 Conventional Long Hauler

As conventional model, a twelve-gear 36-ton long hauler with a 16 liter diesel engine has been chosen as a good representation for the average size of a long hauler.

#### 3.1.1 Vehicle parameters

The vehicle parameters for the long hauler are summarized in Table 3.1. The values are chosen with respect to what is stated in [13]. The mass of the long hauler is chosen w.r.t. the drive cycle, and the 16L combustion engine's torque limits. A truck heavier than 36-ton demands a torque above 3300Nm for the LC\_8 drive cycle.

Parameter	Denomination	Value	Unit
Frontal area	$A_f$	10	m <sup>2</sup>
Drag coefficient	$c_d$	0.8	-
Rolling resistance coefficient	$c_r$	0.008	-
Total long hauler mass	$m_{lh}$	36 000	kg
Wheel radius	$r_w$	0.55	m

*Table 3.1: Vehicle parameters for the long hauler*

### 3.1.2 Gear Box

The gear box in the long hauler is a twelve-gear manual gear box. The efficiency  $\eta_{gb}$  and idling losses  $P_{idle,gb}$  are chosen after [4] and the gear ratios  $\gamma_1 - \gamma_{12}$  and differential gear  $\gamma_{diff}$  are chosen to give desired propulsion through out the gears. Table 3.2 summarizes the parameters for the gear box.

Parameter	Denomination	Value	Unit
Gear box efficiency	$\eta_{gb}$	0.96	-
Idling losses	$P_{idle,gb}$	10	kW
Ratio gear 1	$\gamma_1$	11.729	-
Ratio gear 2	$\gamma_2$	9.211	-
Ratio gear 3	$\gamma_3$	7.094	-
Ratio gear 4	$\gamma_4$	5.571	-
Ratio gear 5	$\gamma_5$	4.348	-
Ratio gear 6	$\gamma_6$	3.414	-
Ratio gear 7	$\gamma_7$	2.698	-
Ratio gear 8	$\gamma_8$	2.118	-
Ratio gear 9	$\gamma_9$	1.632	-
Ratio gear 10	$\gamma_{10}$	1.281	-
Ratio gear 11	$\gamma_{11}$	1	-
Ratio gear 12	$\gamma_{12}$	0.785	-
Differential gear	$\gamma_{diff}$	3.2	-

**Table 3.2:** Gear box parameters

### 3.1.3 Combustion Engine

The 16 liter diesel engine chosen for the conventional powertrain has the maximum torque and power curve shown in Figure 3.1. The engine has at 1300 RPM the maximum torque of 3300Nm and a maximum power of 450kW. The parameters used for the engine geometry is summarized in Table 3.3. The values used for bore  $B$  and stroke  $S$  are from Volvo's D16 engine [15]. The gas exchange losses  $p_{me0}$  and auxiliary losses  $P_{ce,aux}$  are chosen with respect from [4].

Parameter	Denomination	Value	Unit
Displacement	$V_d$	16	dm <sup>3</sup>
Bore	$B$	144	mm
Stroke	$S$	165	mm
Gas exchange losses	$p_{me0}$	$2 \cdot 10^5$	Pa
Auxiliary losses	$P_{ce,aux}$	1000	W

**Table 3.3:** Parameters for the 16 liter diesel engine

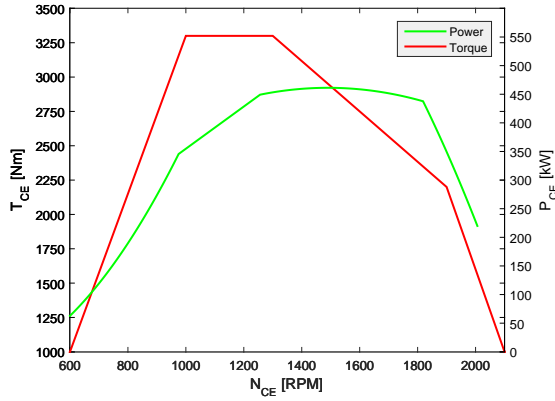


*Figure 3.1: 16L torque curve.*

## 3.2 Parallel Hybrid Long Hauler

The implementation of the parallel hybrid long hauler with its smaller engine (downsizing), assisting electric motor and battery is made to resemble the conventional long hauler in terms of driveability.

### 3.2.1 Downsizing

When using a hybrid driveline, one of the advantages is to make the engine smaller and use the electric motor for power assistance when the combustion engine is not sufficient.

The 13 liter diesel engine has the maximum torque and power curve shown in Figure 3.2. The downsized engine has a maximum torque of 2700Nm and 395kW at 1400 RPM. The parameters used for the engine geometry is summarized in Table 3.4. The values used for bore  $B$  and stroke  $S$  are from Volvo's D13 engine [16].

The downsizing reduces the weight with 1.2 kg/kW according to [14].

Parameter	Denomination	Value	Unit
Displacement	$V_d$	13	$\text{dm}^3$
Bore	$B$	131	mm
Stroke	$S$	158	mm
Gas exchange losses	$p_{me0}$	$1.6 \cdot 10^5$	Pa
Auxiliary losses	$P_{ce,aux}$	1000	W
Reduced weight	$P_{ce,aux}$	75	kg

**Table 3.4:** Parameters for the 13 liter diesel engine

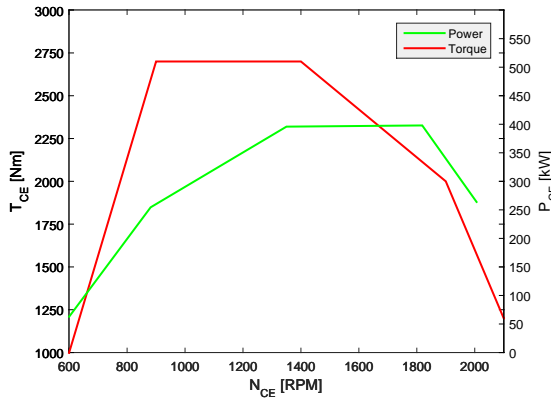


**Figure 3.2:** 13L torque curve.

### 3.2.2 Electric sizing

For a hybrid vehicle, sizing of the electric components is a crucial part in optimizing the fuel consumption. The important trade-off is between not having a too large battery, which adds weight and takes up space otherwise usable for cargo - or a too small battery which depletes in the middle of a hill where assistance is needed.

#### Electric Motor

The electric motor used for the hybrid configuration is chosen given the 13 liter combustion engine with a maximum torque of 2700Nm. For the powertrain to have the same maximum torque available, a 600Nm electric motor torque is chosen. With the scale factor  $\frac{600}{70}$  the desired torque curve in Figure 3.3 is obtained. Table 3.5 summarizes the parameter values for the electric motor.

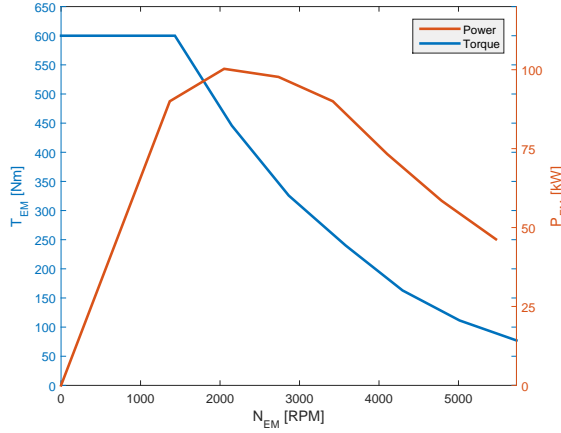


**Figure 3.3:** Torque and power curve for the 600Nm electric motor.

Parameter	Denomination	Value	Unit
Scaling factor	scale_EM	$\frac{600}{70}$	-
Auxiliary losses	$P_{em,aux}$	0	W
Weigh of motor	$m_{em}$	150	kg
Inertia	$J_{em}$	$0.1 \cdot \text{scale\_EM}$	$\text{kg} \cdot \text{m}^2$

**Table 3.5:** Electric motor parameters

### Battery

The battery is sized after the size of the electric motor. With the total battery capacity  $Q_0 = 100\text{Ah}$ , the electric motor can be driven at maximum power ( $I_{bat} = 300$ ) for 20 minutes. Table 3.6 shows all the parameter values used in the battery model.

Parameter	Denomination	Value	Unit
Total capacity	$Q_0$	100	Ah
Open circuit voltage	$U_{oc}$	600	V
Inner resistance	$R_i$	0.75	$\Omega$
Maximum current	$I_{bat,max}$	300	A
Initial SOC	$SOC_{initial}$	60	%
Weigh of battery	$m_{bat}$	330	kg

**Table 3.6:** Parameter values for the battery.



# 4

---

## Controller

One of the key advantages with a hybrid powertrain is the ability to split the torque between the combustion engine and the electric motor. This function hence requires the use of a controller. In this chapter the two types of control strategies used in this thesis are described.

### 4.1 Equivalent Consumption Minimization Strategy

ECMS is a strategy in which the optimization problem is to minimize the sum of power from the fuel and battery [4]. Since these powers are not comparable finding an equivalence factor  $\lambda_{ECMS}$  is required. The equivalence factor converts battery power to the equivalent amount of fuel power needed to keep a charge-sustaining control strategy, making sure that the final state of charge is equal to the initial. If the final state of charge is lower or greater than the initial the fuel consumption cannot be compared completely.

Firstly, in order to have an optimization problem, a varying set of possible output torques need to be calculated. The optimal output w.r.t. to the function to optimize  $H$  is then selected. With the parallel configuration the electric motor and the combustion engine are mechanically coupled through the gear box and thus the following relationships must hold

$$\omega = \omega_{gb} = \omega_{ce} = \omega_{em} \quad (4.1)$$

the angular velocities at the gear box, electric motor and combustion engine all need to be equal and

$$T_{req} = T_{ce} + T_{em} \quad (4.2)$$

the torque split between the combustion engine and electric motor. It is this split which needs to be controlled in an efficient way.

The inputs and outputs of the ECMS controller are

<b>Input variables</b>	Denomination	Unit
Angular velocity	$\omega$	rad/s
Angular acceleration	$\dot{\omega}$	rad/s <sup>2</sup>
Required torque	$T_{req}$	Nm
Equivalence factor	$\lambda_{ECMS}$	-
<b>Output variables</b>		
Combustion engine torque	$T_{ce}$	Nm
Electric motor torque	$T_{em}$	Nm

**Table 4.1:** ECMS controller inputs and outputs

In the controller, constant values for the efficiencies are assumed for simplicity according to Table 4.2.

Efficiency	Denomination	Value
Combustion engine	$\eta_{ce}$	0.4
Electric motor	$\eta_{em}$	0.8

**Table 4.2:** Efficiency assumptions for the ECMS controller

Substituting (2.25) in (2.29) yields

$$T_{em} = \frac{U_{oc} \cdot I_{bat} - R_i \cdot I_{bat}^2}{\omega} \cdot \eta_{em}^{\text{sign}(I_{bat})} \quad (4.3)$$

where the "sign" is used because of the constant efficiency on the electric motor. A negative  $I_{bat}$  meaning that the motor is used as a generator. With (4.2)  $T_{ce}$  is obtained by

$$T_{ce} = T_{req} - T_{em} \quad (4.4)$$

This means that both  $T_{em}$  and  $T_{ce}$  only depend on the variation in the battery current  $I_{bat}$ . By creating an array

$$-I_{bat,max} : I_{step} : I_{bat,max}$$

all possible torque split outputs can be calculated with (4.3) and (4.4) with the desired accuracy decided by  $I_{step}$ , bigger steps will yield a quicker controller with lower performance and smaller steps the opposite. All these calculated outputs are not feasible by the combustion engine and the electric motor, therefore limitations are needed. The following checks are made

$$\left\{ \begin{array}{l} -T_{em,max} \leq T_{em} \leq T_{em,max} \\ -P_{em,max} \leq P_{em} \leq P_{em,max} \\ T_{ce} \leq T_{ce,max} \end{array} \right.$$

with the  $T_{em,max}$ ,  $P_{em,max}$  and  $T_{ce,max}$  shown in Figure 2.6 and 3.2 respectively. The non-feasible torques are removed and the resulting minimization problem is expressed in hamiltonian form as

$$\begin{aligned} H &= P_f + \lambda_{ECMS} \cdot P_{ech} \\ I^* &= \arg \min H \end{aligned} \quad (4.5)$$

where  $P_f$  is the power from the fuel,  $P_{ech}$  is the power in the battery,  $I^*$  is the current which minimizes H and  $\lambda_{ECMS}$  the equivalence factor.

Since the hamiltonian depends on the variation in state of charge and not the state of charge itself one can assume that  $\lambda_{ECMS}$  is constant for the optimal path [4]. The optimal  $\lambda_{ECMS}$  is found by a numerical search where simulations are done with a rising lambda until a charge sustaining value for  $\lambda_{ECMS}$  is achieved. The power from the fuel can be calculated using the feasible engine torques in

$$P_f = \dot{m}_f \cdot q_{LHV} = \frac{\omega_{ce}}{\eta_{ce}} (T_{ce} + J_{ce} \cdot \dot{\omega}_{ce} + \frac{P_{me0} \cdot V_d}{4\pi}) \quad (4.6)$$

and the power in the battery as follows with the feasible currents

$$P_{ech} = -\dot{q} \cdot Q_0 \cdot U_{oc} = I_{bat} \cdot U_{oc} \quad (4.7)$$

The minimizing current  $I^*$  from (4.5) is then used in (4.3) and (4.4) to get the torque split which the controller is giving as output.

When doing an analytic analysis of the minimization problem in (4.5) and substituting (4.3),(4.4),(4.6) and (4.7) into it the result is the following hamiltonian

$$\begin{aligned} H &= \frac{\omega}{\eta_{ce}} (T_{req} - \frac{U_{oc} \cdot I_{bat} - R_i \cdot I_{bat}^2}{\omega} \cdot \eta_{em}^{\text{sign}(U_{oc} \cdot I_{bat} - R_i \cdot I_{bat}^2)}) \\ &+ J_{ce} \cdot \dot{\omega} + \frac{P_{me0} \cdot V_d}{4\pi}) + \lambda_{ECMS} \cdot U_{oc} \cdot I_{bat} \end{aligned} \quad (4.8)$$

Finding the minimum value of the hamiltonian is done by setting the derivative equal to zero.

$$\frac{\partial H}{\partial I_{bat}} = 0 \quad (4.9)$$

Since there is a sign in the hamiltonian there are two cases, one for positive values of  $I_{bat}$  and one for negative values.

**case**  $I_{bat} > 0$

$$\frac{\partial H}{\partial I_{bat}} = \frac{\partial}{\partial I_{bat}} \left( \frac{\omega}{\eta_{ce}} \left( T_{req} - \frac{U_{oc} \cdot I_{bat} - R_i \cdot I_{bat}^2}{\omega} \cdot \eta_{em} + J_{ce} \cdot \dot{\omega} + \frac{p_{me0} \cdot V_d}{4\pi} \right) + \lambda_{ECMS} \cdot I_{bat} \cdot U_{oc} \right) \quad (4.10)$$

By taking the derivative and some rewriting one gets the current  $I^*$  which is the one yielding the optimal control

$$I^* = \frac{U_{oc}}{2 \cdot R_i} \left( 1 - \frac{\eta_{ce}}{\eta_{em}} \cdot \lambda_{ECMS} \right) \quad (4.11)$$

Since  $I_{bat} > 0$  and all parameters are constants it yields the criteria that  $\lambda_{ECMS} < \frac{\eta_{em}}{\eta_{ce}} = 2$  using the assumed constant efficiencies.

**case**  $I_{bat} < 0$

$$\frac{\partial H}{\partial I_{bat}} = \frac{\partial}{\partial I_{bat}} \left( \frac{\omega}{\eta_{ce}} \left( T_{req} - \frac{U_{oc} \cdot I_{bat} - R_i \cdot I_{bat}^2}{\omega \cdot \eta_{em}} + J_{ce} \cdot \dot{\omega} + \frac{p_{me0} \cdot V_d}{4\pi} \right) + \lambda_{ECMS} \cdot I_{bat} \cdot U_{oc} \right) \quad (4.12)$$

as in the previous case one gets the following optimal current

$$I^* = \frac{U_{oc}}{2 \cdot R_i} (1 - \eta_{ce} \cdot \eta_{em} \cdot \lambda_{ECMS}) \quad (4.13)$$

since  $I_{bat} < 0$  and all parameters are constants it yields the criteria that  $\lambda_{ECMS} > \frac{1}{\eta_{em} \cdot \eta_{ce}} = 3.125$  using the assumed constant efficiencies.

## 4.2 Heuristic Controller

For the heuristic controller a simple rule based controller is designed for the parallel hybrid. Heuristic controllers are widely used by companies for powertrain, engine and transmission control [3]. Reasons for this are because they are easy to implement, easy to tune for less complex systems by changing the thresholds in the rules and also that they are computationally fast. The negative thing about heuristic controllers is that they are suboptimal, they depend heavily on the driving conditions and as a result of this they do not always give a charge sustaining control.

For the parallel hybrid configuration in Chapter 3, a power assist strategy is used, meaning that the electric motor assists when the combustion engine is not sufficient. The controller is also implemented so that the electric motor is used for regenerative braking and as a generator when the state of charge gets too low. In the later case the combustion engine torque is increased to still match the required torque. When the state of charge gets too high the electric motor is used.

Table 4.3 summarizes the controller's inputs and outputs. The thresholds for the controller are boundaries for the state of charge

$$SOC_{low} = 0.55 \quad SOC_{high} = 0.65$$

<b>Input variables</b>	Denomination	Unit
Vehicle velocity	$v$	m/s
Angular velocity	$\omega$	rad/s <sup>2</sup>
Required torque	$T_{req}$	Nm
State of Charge	$q$	-
<b>Output variables</b>		
Combustion engine torque	$T_{ce}$	Nm
Electric motor torque	$T_{em}$	Nm

**Table 4.3:** Heuristic controller inputs and outputs



# 5

## Results

The results from the model simulations using the configurations in Chapter 3 are shown in this chapter.

### 5.1 Conventional

In Figure 5.1 the top view of the Simulink model for the conventional long hauler is shown. The average simulation time for the conventional model is 3 seconds on a computer with a 1.6 GHz processor and 4GB of RAM.

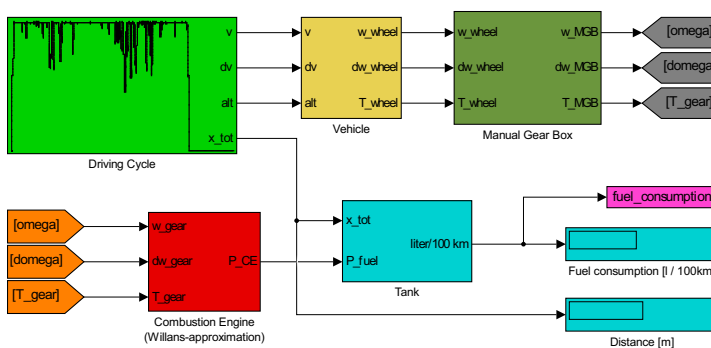


*Figure 5.1: Top view of the conventional long hauler model in Simulink.*

## 5.2 Longitudinal Vehicle Model

The overview of the model for longitudinal propulsion is shown in Figure 5.3 and in Figure 5.2 the simulation results from drive cycle LC\_8 are displayed. In Figure 5.2 one can see that the gravitational forces in subplot four are a big contributor as expected.

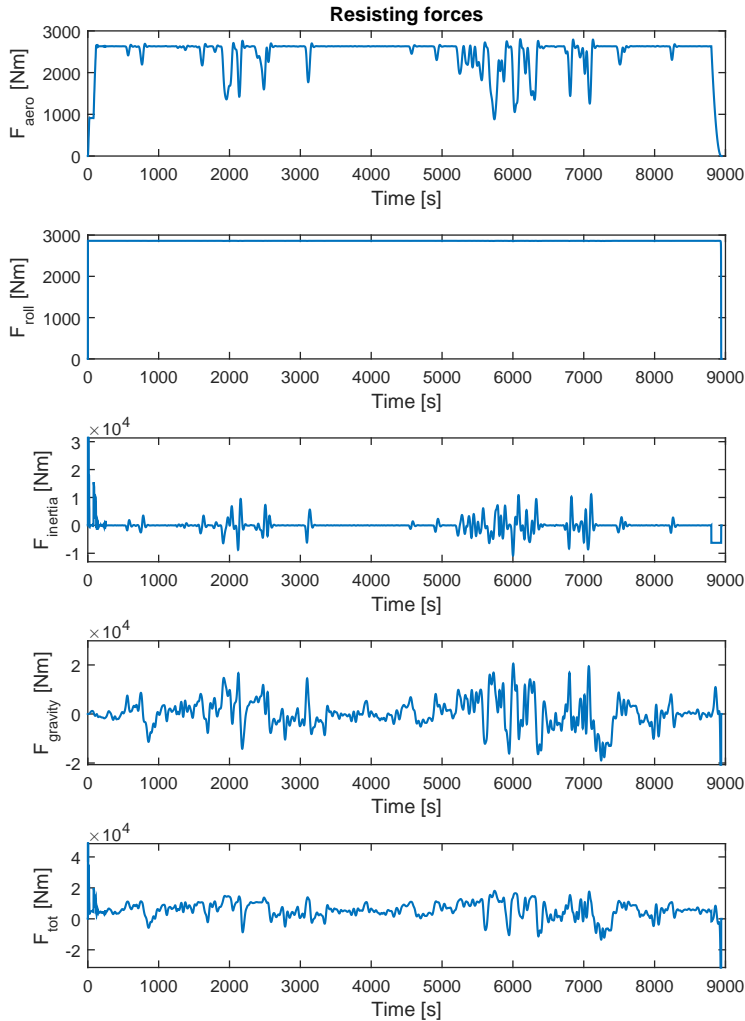


**Figure 5.2:** The resisting forces for the hilliest elevation profile (LC\_8).

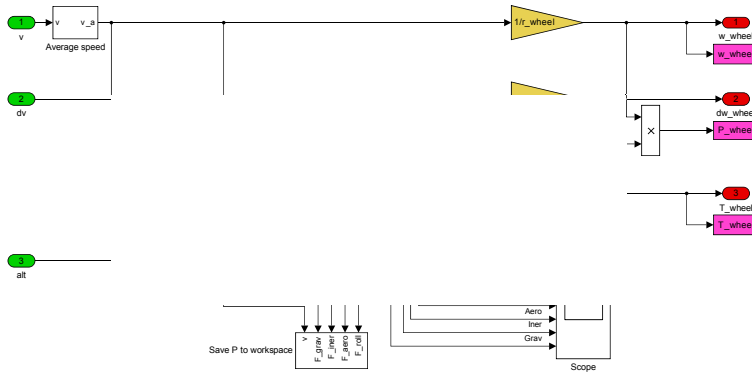


Figure 5.3: Overview of the vehicle model in Simulink.

### 5.3 Gear Box

An overview of the manual gear box model is shown in Figure 5.4.

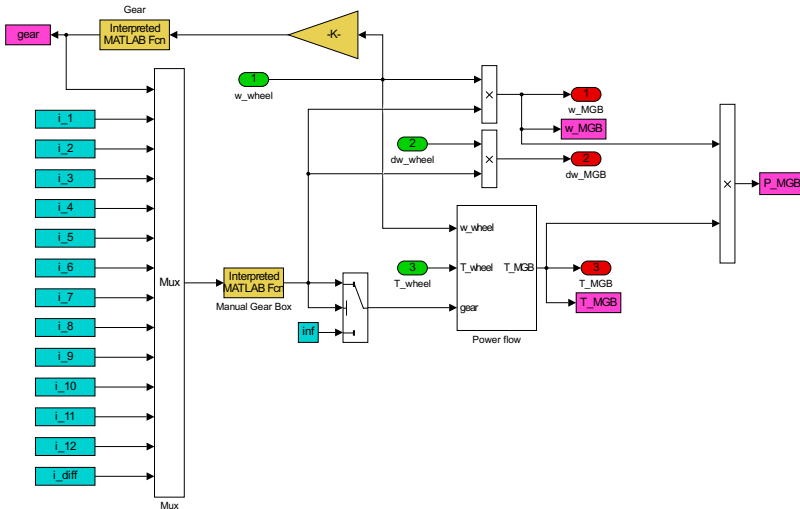


Figure 5.4: Overview of the manual gear box model in Simulink.

#### 5.3.1 Gear Shifting

The simple gear shifting strategy explained in Chapter 2 Section 2.3 results in the plot in Figure 5.5. In the plot it is clear that the long hauler is propelled on the twelfth gear the majority of the cycle.

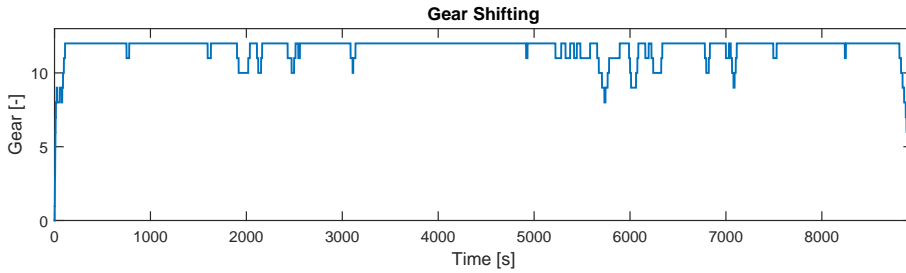


Figure 5.5: The resulting gearshift for the hilliest elevation profile (LC\_8).

## 5.4 Combustion Engine

In Figure 5.6 an overview of the Simulink model is shown and in Figure 5.7 the operation points for the LC\_8 cycle with the 16L diesel engine are depicted. The concentration around 1100 RPM is a result of the simple gear shifting strategy which only depends on vehicle speed and the fact that the long hauler is mostly driven at highway with constant speed 85 km/h in twelfth gear. This area is not where the engine is the most efficient. The engine is at its efficiency peak with a RPM between 1100-1300 and a higher load around 2500Nm - 3200Nm.

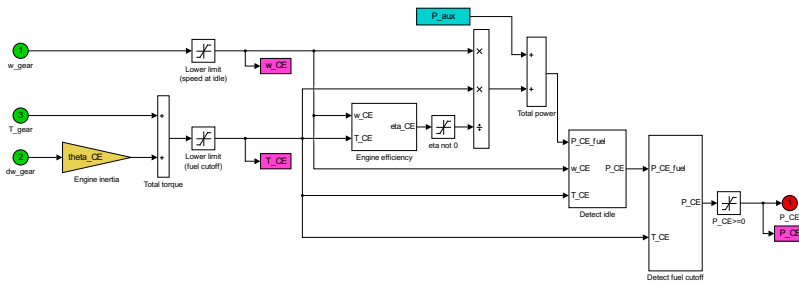
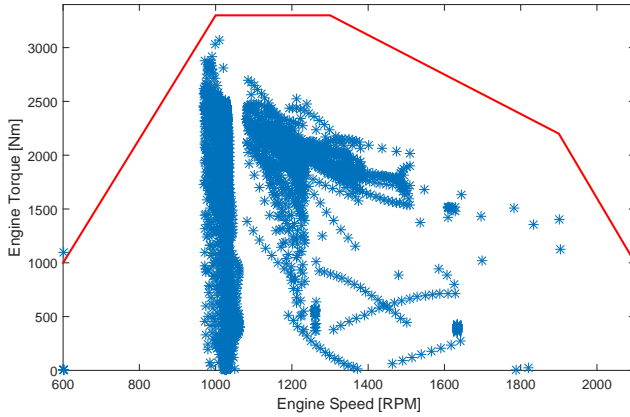


Figure 5.6: Overview of the combustion engine model in Simulink.



**Figure 5.7:** Operation points for the 16 liter diesel engine in the conventional long hauler when driving the LC\_8 drive cycle. Black line represents the maximum torque.

## 5.5 Fuel Consumption

The fuel consumption for the conventional long hauler for each drive cycle are summarized in Table 5.1. For the first cycles the consumption is decreasing which probably depends on that for smaller hills the gravitation is assisting more than it is creating a resistance. After that the trend is a steadily increasing fuel consumption for increasing elevation. The values of the fuel consumption corresponds to reality for a long hauler [1].

Cycle	Fuel Consumption
LC_1	54.76 [l/100km]
LC_2	54.71 [l/100km]
LC_3	54.68 [l/100km]
LC_4	54.96 [l/100km]
LC_5	55.02 [l/100km]
LC_6	55.45 [l/100km]
LC_7	56.16 [l/100km]
LC_8	57.75 [l/100km]

**Table 5.1:** Simulation results for the conventional long hauler.

## 5.6 Parallel Hybrid

In Figure 5.8 the top view of the Simulink model for the parallel hybrid long hauler is shown. The average simulation time for the parallel hybrid is 12 sec-

onds with the ECMS controller and 5 seconds with the heuristic controller on a computer with a 1.6 GHz processor and 4GB of RAM.

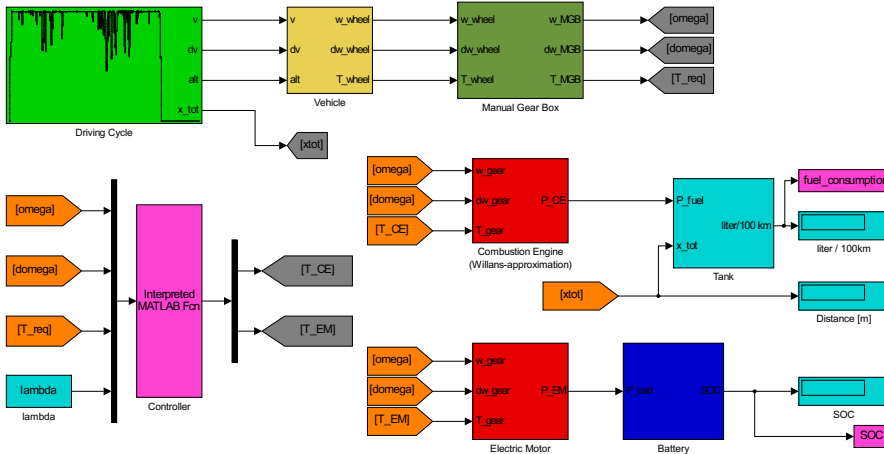


*Figure 5.8: Top view of the parallel hybrid long hauler with the ECMS control.*

### 5.6.1 Downsized Combustion Engine

The downsized 13 liter combustion engine has similar operating points as the 16 liter engine and they are shown in Figure 5.9. This is also an effect of the gear shift strategy.

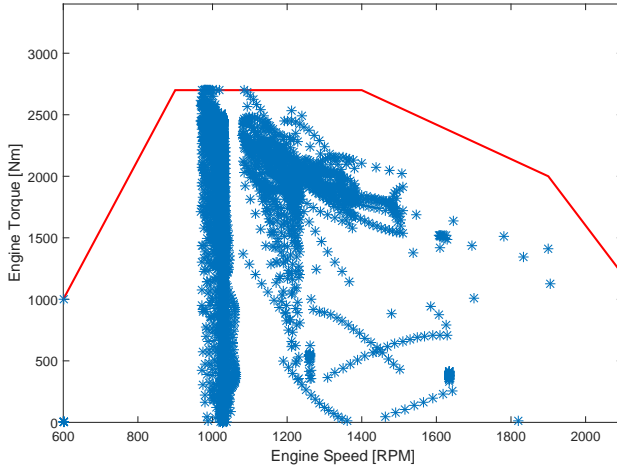


**Figure 5.9:** Operation points for the 13 liter diesel engine in the parallel hybrid long hauler when driving the LC\_8 drive cycle. Black line represents the maximum torque.

### 5.6.2 Electric Motor

The electric motor which is used both as a motor to propel the long hauler and as a generator to recuperate energy has most of its operation points at the 100 [rad/s] area as shown in Figure 5.10. This concentration is due to mostly being driven in twelfth gear and at the constant speed of 85 km/h and following the same gear ratios as the combustion engine. Looking at the efficiency map in Figure 2.5 it is clear that these operation points are not optimal for the electric motor.

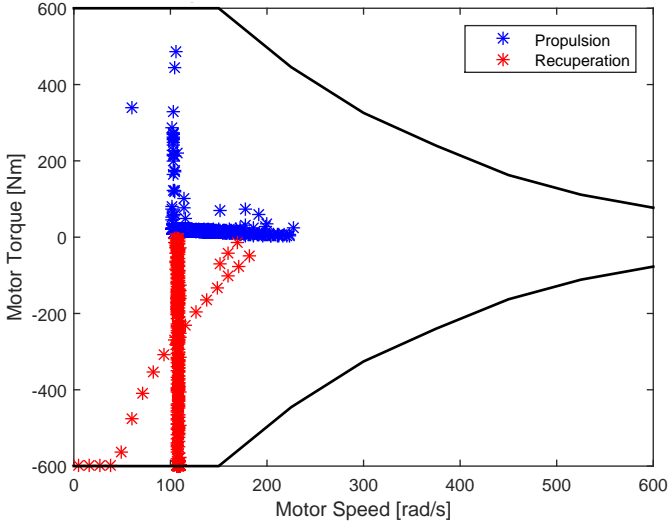


**Figure 5.10:** Operation points for the 600Nm electric motor in the parallel hybrid long hauler when driving the LC\_8 drive cycle. Black lines represent the maximum torque.

## 5.7 Fuel Consumption

The fuel consumption for the hybrid long hauler depends on the choice of controller. In the first section the consumption yielded from the ECMS controller is discussed and the same is done in the second section but for the heuristic controller.

### 5.7.1 ECMS Controller

Firstly the optimal  $\lambda_{ECMS}$  values need to be found. By simulating the model for a set of  $\lambda_{ECMS}$  values, the one that leads to battery charge sustaining (the optimal value) is found. Figure 5.11 depicts the result of such a search made for the LC\_5 drive cycle. In the plot one can see the limit at  $\lambda_{ECMS} = \frac{\eta_{em}}{\eta_{ce}} = 2$  discussed in Chapter 4.

In Figure 5.12, 5.13 and 5.14 the resulting fuel consumption and state of charge variation for drive cycle LC\_8, LC\_5 and LC\_1 are shown. The fourth subplot, showing the state of charge variation indicates a very narrow band in which the battery is used.

The fuel consumptions for each drive cycle are shown in Table 5.2. For the first four cycles there are not enough parts within the cycle for the hybrid to recuperate energy needed for the acceleration in the beginning. This leads to a final SOC lower than the initial and to a lower fuel consumption because the

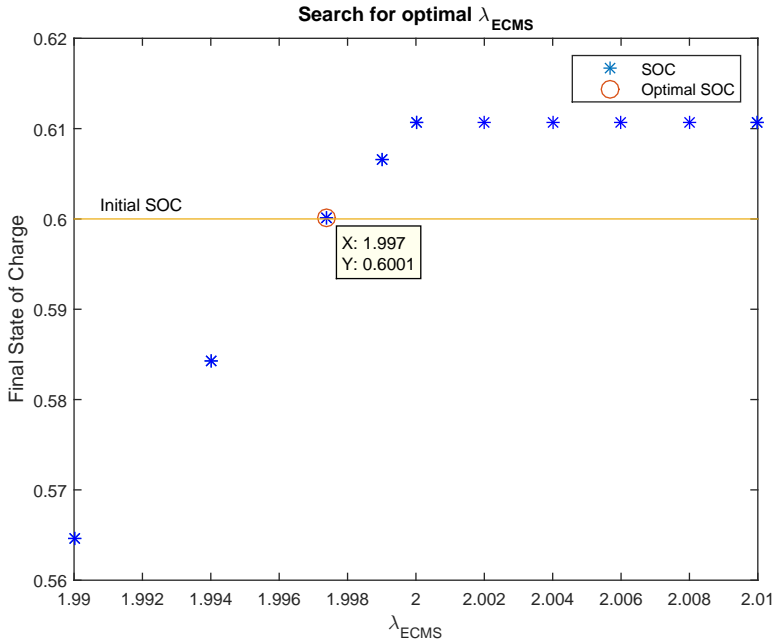


**Figure 5.11:** Search for the optimal equivalence factor for the LC\_5 drive cycle.

battery power has been used instead of the fuel.

Cycle	Final SOC	Fuel Cons.	Conventional Cons.	Improvement
LC_1	59.8%	51.48 [l/100km]	54.76 [l/100km]	5.99 [%]
LC_2	59.8%	51.44 [l/100km]	54.71 [l/100km]	5.98 [%]
LC_3	59.8%	51.42 [l/100km]	54.68 [l/100km]	5.98 [%]
LC_4	59.8%	51.62 [l/100km]	54.96 [l/100km]	6.08 [%]
LC_5	60%	51.67 [l/100km]	55.02 [l/100km]	6.09 [%]
LC_6	60%	51.97 [l/100km]	55.45 [l/100km]	6.28 [%]
LC_7	60%	52.52 [l/100km]	56.16 [l/100km]	6.47 [%]
LC_8	60%	53.99 [l/100km]	57.75 [l/100km]	6.51 [%]

**Table 5.2:** Simulation results for the parallel hybrid long hauler with ECMS controller.

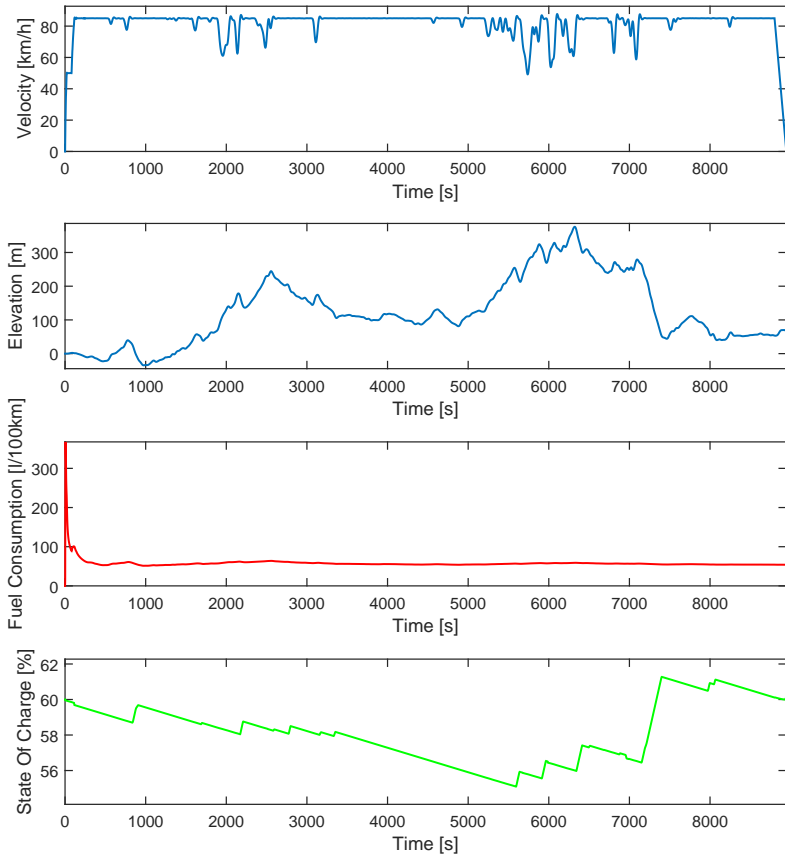


**Figure 5.12:** Resulting fuel consumption (lower middle subplot) and SOC variation (bottom subplot) for the ECMS controller from the Lyon-Clermont drive cycle with the 375m (LC\_8) maximum elevation profile (upper middle subplot).

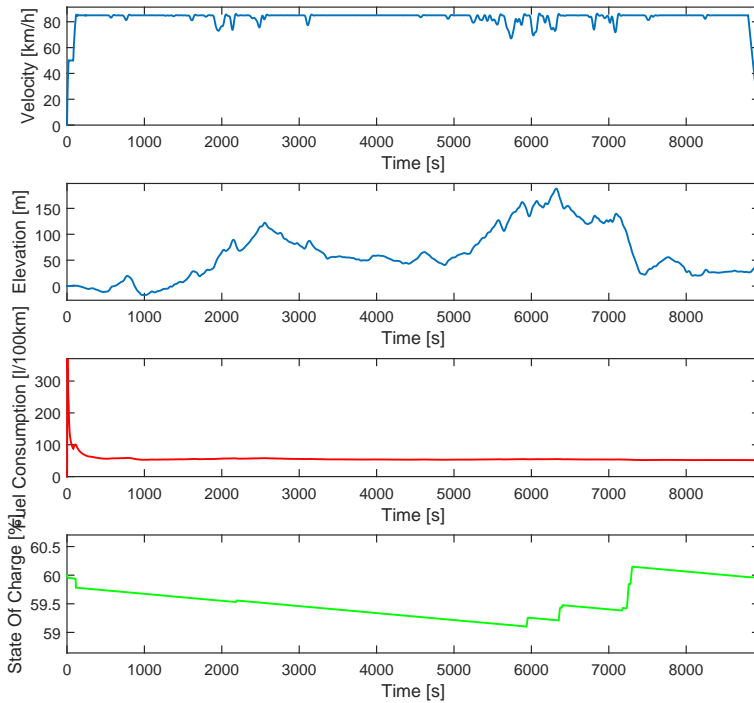


**Figure 5.13:** Resulting fuel consumption (lower middle subplot) and SOC variation (bottom subplot) for the ECMS controller from the Lyon-Clermont drive cycle with the 190m (LC\_5) elevation profile (upper middle subplot).

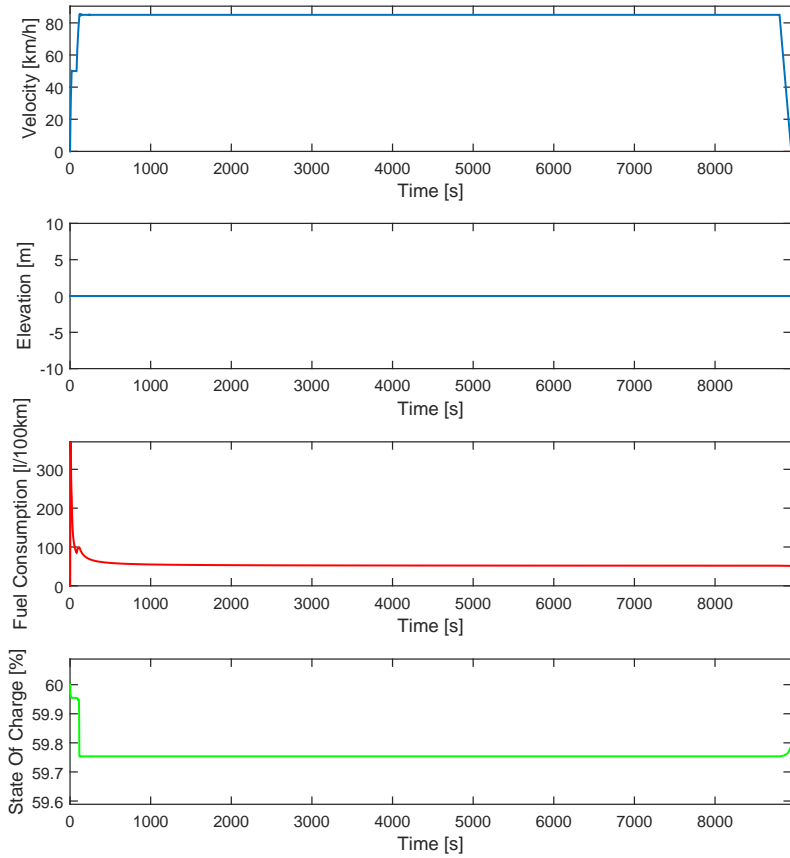


**Figure 5.14:** Resulting fuel consumption (lower middle subplot) and SOC variation (bottom subplot) for the ECMS controller from the Lyon-Clermont drive cycle with a flat (LC\_1) elevation profile (upper middle subplot).

### 5.7.2 Heuristic Controller

The heuristic controller shows a large dependence in the elevation profile. The way the controller is designed is to recuperate as much energy as possible. In Figure 5.17, a charge sustaining control is achieved. When there is too much slopes the controller yields a control that charges the battery too much and obtaining a final SOC which is higher than the initial. This is seen in Figure 5.16 and Figure 5.15. For the comparison to be as accurate as possible this is not good, since extra fuel has then been used to charge the battery. The results for all the drive cycles are summarized in Table 5.3.

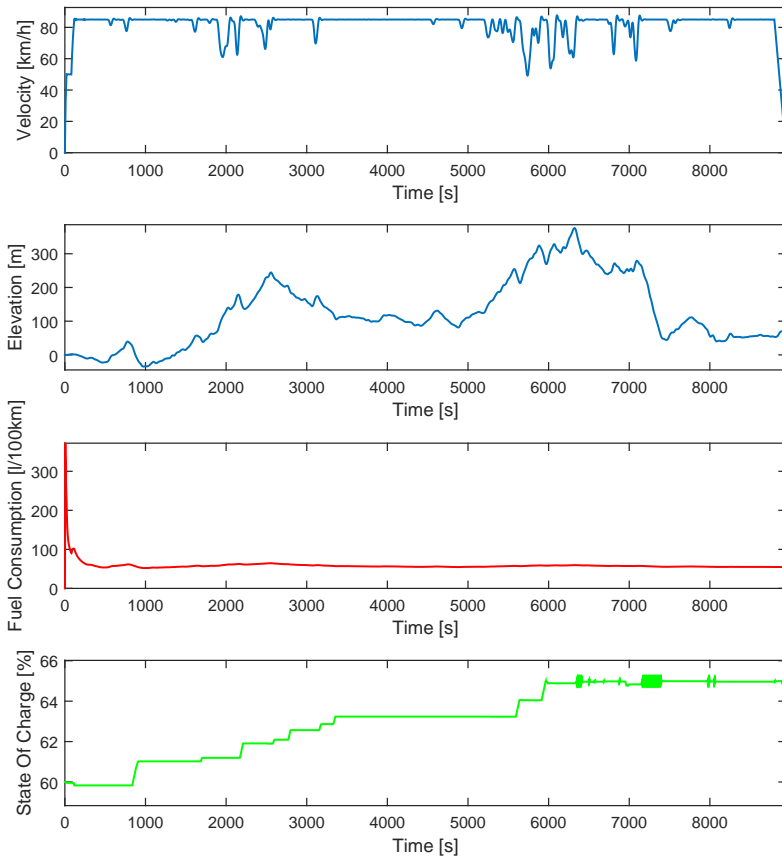


**Figure 5.15:** Resulting fuel consumption (lower middle subplot) and SOC variation (bottom subplot) for the heuristic controller from the Lyon-Clermont drive cycle with the 375m (LC\_8) maximum elevation profile (upper middle subplot).

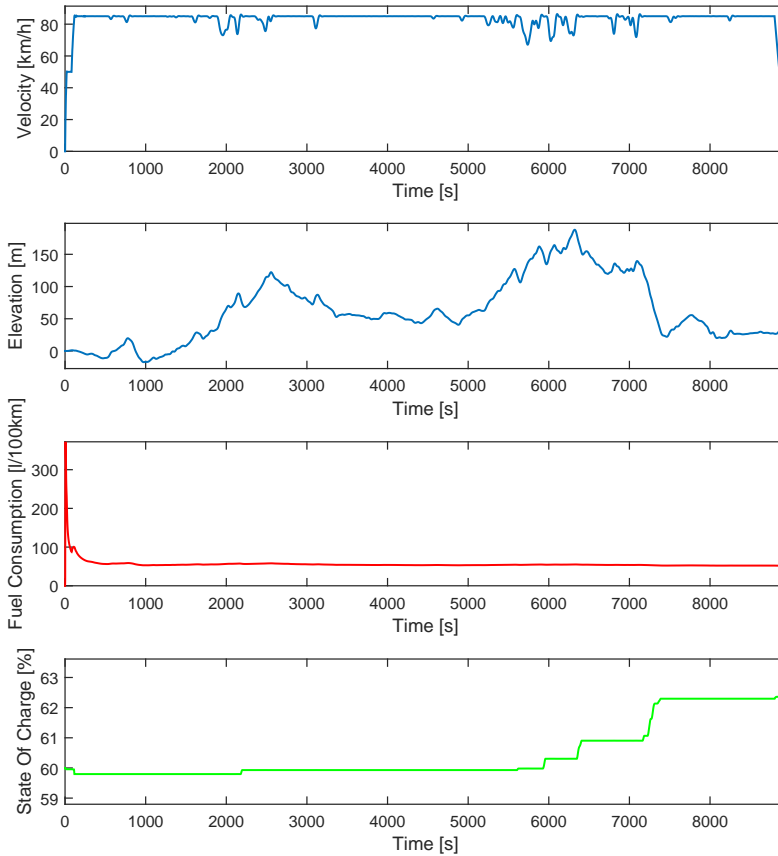


**Figure 5.16:** Resulting fuel consumption (lower middle subplot) and SOC variation (bottom subplot) for the heuristic controller from the Lyon-Clermont drive cycle with the 190m (LC\_5) elevation profile (upper middle subplot).

Cycle	Final SOC	Fuel Cons.	Conventional Cons.	Improvement
LC_1	60.4%	51.48 [l/100km]	54.76 [l/100km]	5.99 [%]
LC_2	60.3%	51.44 [l/100km]	54.71 [l/100km]	5.98 [%]
LC_3	60.1%	51.42 [l/100km]	54.68 [l/100km]	5.97 [%]
LC_4	60.3%	51.65 [l/100km]	54.96 [l/100km]	6.03 [%]
LC_5	62.6%	51.87 [l/100km]	55.02 [l/100km]	5.73 [%]
LC_6	64.9%	52.37 [l/100km]	55.45 [l/100km]	5.57 [%]
LC_7	64.9%	53.02 [l/100km]	56.16 [l/100km]	5.59 [%]
LC_8	64.9%	54.7 [l/100km]	57.75 [l/100km]	5.29 [%]

**Table 5.3:** Simulation results for the parallel hybrid long hauler with heuristic controller.

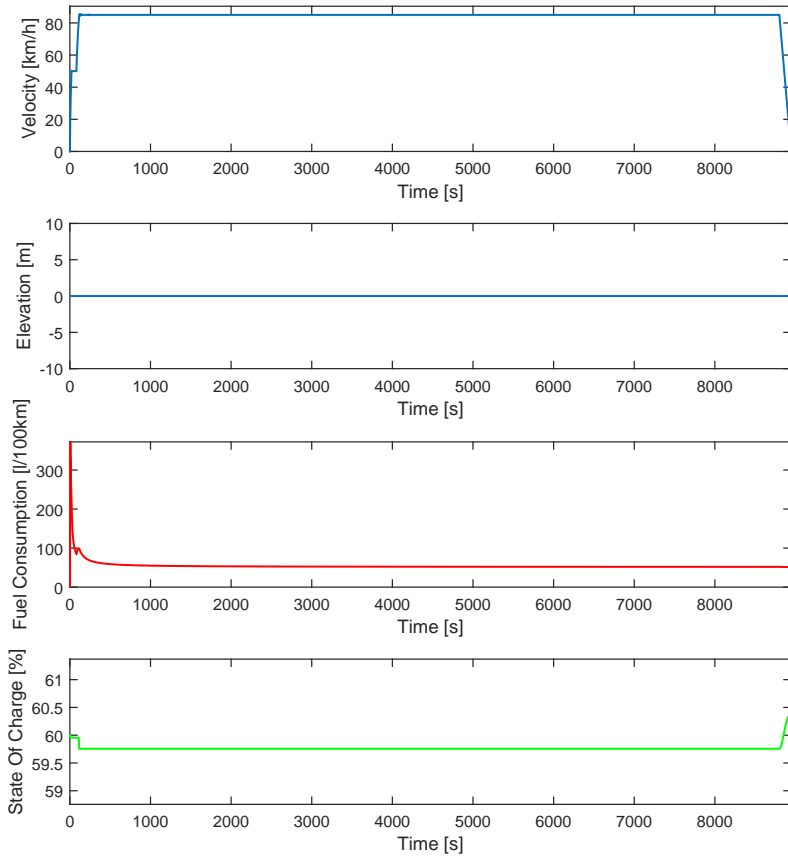


**Figure 5.17:** Resulting fuel consumption (lower middle subplot) and SOC variation (bottom subplot) for the heuristic controller from the Lyon-Clermont drive cycle with a flat (LC\_1) elevation profile (upper middle subplot).

## 5.8 Sensitivity analysis

To fully evaluate how the model behaves a sensitivity analysis is done. This permits to determine the most influential parameters in the model. The vehicle parameters are analysed to see how greatly the choice of them impacts the resulting torque requirements and thus the final fuel consumption. This could show which parameters there are most to gain from by improving. The other parameters are analysed to see how important accurate values are for the model. The analysis was performed using the conventional powertrain for all parameters. The reason for not using the parallel for all is for the need to re-tune the controller for every parameter change. The parameters checked in the analysis are the summarized below.

- Long Hauler weight,  $m_{lh}$
- Frontal area,  $A_f$
- Drag coefficient,  $c_d$
- Roll coefficient  $c_r$
- Wheel radius,  $r_w$
- Engine efficiency,  $\eta_{ce}$
- Gas exchange losses,  $p_{me0}$
- Idle losses for combustion engine,  $P_{ce,idle}$
- Auxiliary losses for combustion engine,  $P_{ce,aux}$
- Inertia for combustion engine,  $J_{ce}$
- Gear box efficiency,  $\eta_{gb}$
- Idle losses for gear box,  $P_{gb,idle}$

The analysis resulted in the values presented in Table 5.4.

The mass of the long hauler  $m_{lh}$  plays a big role in the forces needed to propel the long hauler so that lowering of the mass results in reduced fuel consumption is trivial.

The frontal area  $A_f$  and the drag coefficient  $c_d$  works together in (2.6) so that they have similar effect on the fuel consumption seems reasonable.

All vehicle parameters show that smaller variation in them make differences in the same size as the hybrid configurations like the results in [10] also showed. The choice of engine inertia  $J_{ce}$ , the idling losses  $P_{ce,idle}$  and the auxiliarty losses  $P_{ce,aux}$  for the combustion engine shows small variations in the resulting fuel consumption. The gas exchange losses  $p_{me0}$  do effect when they vary quite a lot as the results show.

Parameter	Value		Fuel Cons.	$\Delta$ Fuel Cons.
$m_{lh}$	32	[ton]	54.86 [l/100km]	-5 [%]
	34	[ton]	56.28 [l/100km]	-2.5 [%]
$A_f$	8	[m <sup>2</sup> ]	54.41 [l/100km]	-5.8 [%]
	12	[m <sup>2</sup> ]	61.15 [l/100km]	+5.9 [%]
$c_d$	0.6	[-]	53.57 [l/100km]	-7,3 [%]
	1	[-]	62.01 [l/100km]	+7,4 [%]
$c_r$	0.006	[-]	52.99 [l/100km]	-8.2 [%]
	0.01	[-]	62.62 [l/100km]	+8.4 [%]
$r_w$	0.5	[m]	59.28 [l/100km]	+2.6 [%]
	0.6	[m]	56.57 [l/100km]	-2.1 [%]
$\eta_{ce}$	0.38	[-]	60.79 [l/100km]	+5.3 [%]
	0.42	[-]	55.01 [l/100km]	-4.8 [%]
$p_{me0}$	1.5e5	[Pa]	55.78 [l/100km]	-3.4 [%]
	2.5e5	[Pa]	59.73 [l/100km]	+3.4 [%]
$P_{ce,idle}$	3	[kW]	57.76 [l/100km]	0 [%]
	9	[kW]	57.76 [l/100km]	0 [%]
$P_{ce,aux}$	0	[kW]	57.65 [l/100km]	-0.2 [%]
	2	[kW]	57.87 [l/100km]	+0.2 [%]
$J_{ce}$	0.1	[kg · m <sup>2</sup> ]	57.76 [l/100km]	0 [%]
	1	[kg · m <sup>2</sup> ]	57.76 [l/100km]	0 [%]
$\eta_{gb}$	0.94	[-]	58.74 [l/100km]	+1.7 [%]
	0.98	[-]	56.81 [l/100km]	-1.6 [%]
$P_{gb,idle}$	8	[kW]	57.16 [l/100km]	-1 [%]
	12	[kW]	58.37 [l/100km]	+1.1 [%]

**Table 5.4:** Simulation results for the sensitivity analysis in comparison towards the set parameters in Chapter 3 for the conventional long hauler and the LC\_8 drive cycle.



# 6

---

## Conclusions

The conclusions to be drawn from the results in Chapter 5 are that there are benefits with a parallel hybridization of a heavy-duty long hauler. The resulting improvements seem to be dependent on the elevation profile of the road. The most influential part seems to be the downsizing of the combustion engine. This seems reasonable and downsizing the engine further is probably possible.

Results from the simulations show that the simple gear shift strategy is not optimal and improvements in it can be made. A gear shifting model taking the torque request in consideration as well, would do a lot for the resulting operation points within the combustion engine and electric motor.

The ECMS controller seemed to be the better controller since for hilly profiles the ECMS controller shows a better behaviour due to an efficient optimization of the torque split. This because there where no resulting increase in the SOC which means that no fuel where wasted charging the battery.

The results are similar to the results achieved in [7] and [10] and this shows that the results are reasonable. The thesis has not gone in depth about costs of the hybridization but in [10] where the costs also are used for comparison they show that changes with the conventional long haulers parameters such as drag coefficient  $c_d$  and roll coefficient  $c_r$  are more beneficial.

### 6.1 Future Work

Because of the time frame some things were not possible to investigate but would have been interesting for the thesis. Firstly, a configuration containing supercapacitors together with the battery to be able to recuperate larger power peaks like described in [17]. With a configuration using supercapacitors the assumption in Chapter 4 that the hamiltonian in (4.5) only depends on the variation in state of charge does not hold, yielding a more complex controller or only the heuristic

controller. Secondly, overall the models used are very simple and more complex models would give more accurate and trustworthy results. For this to be possible a parameterization of the model needs to be done and for this measured data is needed.

Finally, an interesting approach would be to consider the construction costs and use that information in the evaluation, to see if hybridization is beneficial.

---

## Bibliography

- [1] Oak Ridge Laboratory. *Transportation Energy Data Book*. 33 edition, July 2014. Cited on pages 1 and 35.
- [2] *OECD Economic Outlook*. Organisation for Economic Cooperation and Development, 2012. Cited on page 1.
- [3] Rudy Smaling Haoran Hu and Simon J. Baseley. *Advanced Hybrid Powertrains for Commercial Vehicles*. SAE International, 2012. Cited on pages 1, 3, and 28.
- [4] L. Guzzella and A. Sciarretta. *Vehicle Propulsion Systems*. Springer-Verlag, 2 edition, 2007. Cited on pages 2, 12, 15, 20, 25, and 27.
- [5] Y. J. CHUNG E. Y. LEE B. SUH S. B. HAN, Y. H. CHANG and A. FRANK. Fuel economy comparison of conventional drive trains series and parallel hybrid electric step vans. *International Journal of Automotive Technology*, 10(2):235–240, 2009. Cited on page 6.
- [6] Chih-Wei Hung Chih-Keng Chen, Tri-Vien Vu and Chih-Jer Lin. Modeling and simulation study of a series hydraulic hybrid vehicle. *Applied Mechanics and Materials*, 284-287:834–838, January 2013. Cited on page 6.
- [7] Matthias Jönsson and Milen Kourtev. Predictive energy management for a mild hybrid long haul truck. Master’s thesis, CHALMERS UNIVERSITY OF TECHNOLOGY, 2010. Cited on pages 6 and 49.
- [8] Erik Hellström. *Look-ahead Control of Heavy Vehicles*. PhD thesis, Linköping University, 2010. Cited on page 6.
- [9] Antoine Delorme Dominik Karbowski and Aymeric Rousseau. Modeling the hybridization of a class-8 line-haul. *SAE International*, 2010. Cited on page 7.
- [10] Fereydoon Diba and Ebrahim Esmailzadeh. A new parallel-series configuration for hybridization of a line-haul truck. University of Ontario Institute of Technology, Faculty of Science and Applied Science, Oshawa, ON, Canada,

- 85458, Piscataway, NJ USA; Detroit, MI USA: IEEE Country of Publication: USA, 2013. Cited on pages 7, 46, and 49.
- [11] Andrew Burke Hengbing Zhao and Marshall Miller. Analysis of class 8 truck technologies for their fuel savings and economics. *Transportation Research Part D*, 23:55–63, August 2013. Cited on page 7.
- [12] A. Amstutz L. Guzzella. *The QSS Toolbox Manual*, 2005. Cited on pages 9, 14, and 16.
- [13] Jo Yung Wong. *Theory of Ground Vehicles*. John Wiley & Sons, 2008. Cited on pages 12 and 19.
- [14] Lars Eriksson. *TSFS03 Vehicle Propulsion Systems Hand-in assignments*. <http://www.vehicular.isy.liu.se/Edu/Courses/TSFS03/compendium.pdf>. Cited on pages 17 and 21.
- [15] Volvo Trucks. D16 family. 2013. Cited on page 20.
- [16] Volvo Trucks. D13 family. 2013. Cited on page 21.
- [17] P. Bartholomeüs B. Barbedette R. Sadoun, N. Rizoug and P. Le Moigne. Optimal sizing of hybrid supply for electric vehicle using li-ion battery and supercapacitor. Cited on page 49.



## Upphovsrätt

Detta dokument hålls tillgängligt på Internet — eller dess framtida ersättare — under 25 år från publiceringsdatum under förutsättning att inga extraordinära omständigheter uppstår.

Tillgång till dokumentet innebär tillstånd för var och en att läsa, ladda ner, skriva ut enstaka kopior för enskilt bruk och att använda det oförändrat för icke-kommersiell forskning och för undervisning. Överföring av upphovsrätten vid en senare tidpunkt kan inte upphäva detta tillstånd. All annan användning av dokumentet kräver upphovsmannens medgivande. För att garantera äktheten, säkerheten och tillgängligheten finns det lösningar av teknisk och administrativ art.

Upphovsmannens ideella rätt innefattar rätt att bli nämnd som upphovsman i den omfattning som god sed kräver vid användning av dokumentet på ovan beskrivna sätt samt skydd mot att dokumentet ändras eller presenteras i sådan form eller i sådant sammanhang som är kränkande för upphovsmannens litterära eller konstnärliga anseende eller egenart.

För ytterligare information om Linköping University Electronic Press se förlagets hemsida <http://www.ep.liu.se/>

## Copyright

The publishers will keep this document online on the Internet — or its possible replacement — for a period of 25 years from the date of publication barring exceptional circumstances.

The online availability of the document implies a permanent permission for anyone to read, to download, to print out single copies for his/her own use and to use it unchanged for any non-commercial research and educational purpose. Subsequent transfers of copyright cannot revoke this permission. All other uses of the document are conditional on the consent of the copyright owner. The publisher has taken technical and administrative measures to assure authenticity, security and accessibility.

According to intellectual property law the author has the right to be mentioned when his/her work is accessed as described above and to be protected against infringement.

For additional information about the Linköping University Electronic Press and its procedures for publication and for assurance of document integrity, please refer to its www home page: <http://www.ep.liu.se/>